A Journal of the Gesellschaft Deutscher Chemiker

Angewandte International Edition GDCh Chemie

www.angewandte.org

Accepted Article

Title: Nickel-Catalyzed Migratory Hydrocyanation of Internal Alkenes: Unexpected Diastereomeric-Ligand-Controlled Regiodivergence

Authors: Jihui Gao, Mingdong Jiao, Jie Ni, Rongrong Yu, Gui-Juan Cheng, and Xianjie Fang

To be cited as: *Angew. Chem. Int. Ed.* 10.1002/anie.202011231

Link to VoR: https://doi.org/10.1002/anie.202011231

WILEY-VCH

10.1002/anie.202011231

WILEY-VCH

Nickel-Catalyzed Migratory Hydrocyanation of Internal Alkenes: Unexpected Diastereomeric-Ligand-Controlled Regiodivergence

Jihui Gao[+],[a] Mingdong Jiao[+],[a] Jie Ni[+],[b] Rongrong Yu,[a] Gui-Juan Cheng,*[b] and Xianjie Fang*[a]

Abstract: *We herein report a regiodivergent nickel-catalyzed hydrocyanation of a broad range of internal alkenes involving the chain-walking process. When appropriate diastereomeric biaryl diphosphite ligands are applied, the same starting materials can be converted to either linear or branched nitriles with good yields and high regioselectivities. DFT calculations suggested that the catalyst architecture determines the regioselectivity via modulating electronic and steric interactions. In addition, moderate enantioselectivities were observed when branched nitriles were delivered.*

Introduction

Over the past decades, catalytic reactions featuring divergent regio-, chemo- or diastereoselectivities have become an ultimate pursuit by many synthetic chemists because these methodologies provide new access to diverse functionalized products from the same starting materials.[1] The catalytic conversion of one common substrate into different products often hinges on different metal catalysts (Scheme 1a).[2] Despite the preliminary advances in catalytic divergent reactions, this strategy still needs to be further explored, especially in the field of powerful remote chain-walking functionalization towards the construction of C–C[3] and C–X (X = B,[4] O,[5] Si,[6] S,[7] N[8]) bonds. The chain-walking hydrofunctionalization of internal alkenes, however, is still restricted to "unidirectional" events which favors the activation of a single reaction site.[9] More recently, a few but impressively efficient examples have been reported regarding to the switchable and controllable site-selectivity.[10]

Multi-chiral ligands are an important class of chiral ligands which found wide applications in asymmetric metal catalysis.[11] It is often necessary to study the effects of diastereomeric ligands on the reactivity and enantioselectivity when using multi-chiral ligands in catalytic asymmetric reactions.[12] However, the corresponding effects on regioselectivity have received much less attention. This is somewhat counterintuitive, as the diastereomeric ligands have different configurations and thus induce different regioselectivities. We therefore envision that the use of diastereomeric ligands in metal-catalyzed reactions involving a regioselective issue would provide a novel strategy to achieve regiodivergent synthesis (Scheme 1b).

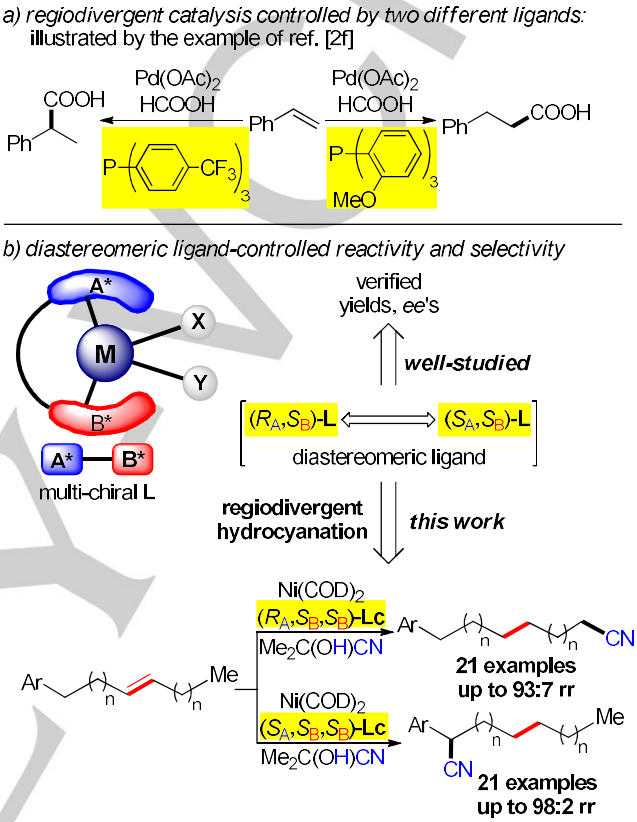

Scheme 1. Background for the development of the current work.

Owing to a perfect atom economy, the catalytic hydrocyanation of alkenes represents one of the most straightforward methods for the preparation of alkyl nitriles, which represent versatile building blocks and intermediates for the chemical, pharmaceutical, and agrochemical industries.[13] Although a numerous of catalytic systems have been developed for the hydrocyanation of alkenes over the past few decades,[14] regioselective isomerization/hydrocyanation of inactivated aliphatic alkenes still represents a challenging topic in this field. In 2018, Studer[15] reported a Pd-catalyzed migratory transfer hydrocyanation of internal alkenes leading to linear nitriles. More recently, Liu[16] and Yang[17] reported a Ni-catalyzed isomerization/hydrocyanation of terminal alkenes that led to branched nitriles. It is worth mentioning that the success of these transformations depends on the Lewis acid when applied. Despite these elegant contributions, catalytic regiodivergent hydrocyanation of internal olefins toward the preparation of linear and branched nitriles, to the best of our knowledge, has not been documented. Herein, we describe the first diastereomeric ligand-controlled chain-walking process for regiodivergent hydrocyanation of internal alkenes, selectively

[a] J. Gao,[+] M. Jiao,[+] R. Yu, Prof. Dr. X. Fang
Shanghai Key Laboratory for Molecular Engineering of Chiral Drugs
Frontiers Science Center for Transformative Molecules
School of Chemistry and Chemical Engineering
Shanghai Jiao Tong University
800 Dongchuan Road, Shanghai 200240, China
E-mail: fangxj@sjtu.edu.cn
[b] J. Ni,[+] Prof. Dr. G.-J. Chen
Warshel Institute for Computational Biology
Shenzhen Key Laboratory of Steroid Drug Development
School of Life and Health Sciences
The Chinese University of Hong Kong (Shenzhen)
Shenzhen, 518172, China
E-mail: chengguijuan@cuhk.edu.cn
[+] These authors contributed equally to this work.
Supporting information and the ORCID identification number(s) for the author(s) of this article can be found under:

producing benzylic and terminal nitriles with high regioselectivities (Scheme 1b).

Results and Discussion

Phosphite ligands have proved to be effective for metal-catalyzed hydrocyanation reactions.[14d,f,g,h,o,p,r] Hence, a series of diastereomeric biaryl diphosphite ligands were prepared according to the general method described in Scheme 2 (see the SI for details). These ligands are derived from commercially available (*S*)-BINOL. Of note, the cost of (*S*)-BINOL is similar to *rac*-BINOL. Diastereomers (R_A,S_B,S_B)-**L** and (S_A,S_B,S_B)-**L** were obtained through the coupling of *rac*-diphenol with [(*S*)-BINOL]PCl. This P–O coupling was barely diastereoselective and the two diastereomers were generated in a *ca*. 1:1.2~1:1.6 ratio. These two diastereomers could be separated through column chromatography, which avoided the otherwise tedious and sometimes difficult resolution steps.

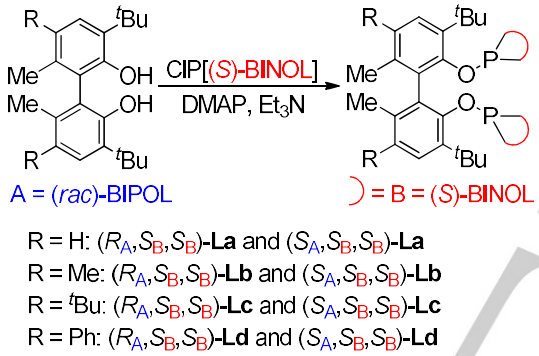

Scheme 2. Preparation of the diastereomeric biaryl diphosphite ligands.

With these diastereomeric biaryl diphosphite ligands, we next studied the regiodivergent migratory hydrocyanation of 1-phenyl-3-hexene (**1a**). With $Me_2C(OH)CN$ as hydrogen cyanide source under nickel catalysis and the diastereomeric biaryl diphosphite ligands, the yield and the regioselectivity of the corresponding nitrile products **2a** and **3a** were examined respectively (Table 1). Herein, the following two characteristics of the ligand effect were observed. 1) These diastereomeric ligands have a dramatic effect on the regioselectivity of the reaction. The (S_A,S_B,S_B)-**L** ligands favored the formation of branched nitrile **2a** with up to 91:9 regioselectivity (Table 1, entries 1−4). Conversely, the regioselectivity was reversed when the (R_A,S_B,S_B)-**L** ligands were employed, and the linear nitrile **3a** were obtained with up to 88:12 regioselectivity (Table 1, entries 5−8). 2) The R substituent strongly influences the yield of the desired nitrile product without affecting the regioselectivity and enantioselectivity of the reaction too much (Table 1, entries 1−8). Notably, the ^{t}Bu-substituted (S_A,S_B,S_B)-**Lc** gave the branched product **2a** in 88% isolated yield with 90:10 regioselectivity (Table 1, entry 3). Meanwhile, the corresponding diastereomeric ligand (R_A,S_B,S_B)-**Lc** afforded the linear product **3a** in 68% isolated yield with 88:12 regioselectivity (Table 1, entry 7). Either lower (Table 1, entries 10 and 12) or higher (Table 1, entries 9 and 11) reaction temperature gave inferior results compared to the reaction run at 80 °C. Lowering or increasing the reaction temperature has almost no effect on the enantioselectivity of the reaction (Table 1, entries 9−10 vs. entry 3).

Table 1: Investigation of the reaction conditions.[a]

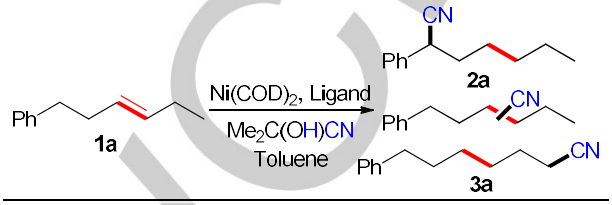

Entry	Ligand	**2a** Yield/%[b]	**3a** Yield/%[b]	rr[d]
1	(S_A,S_B,S_B)-**La**	40(51)[g]	trace	91:9
2	(S_A,S_B,S_B)-**Lb**	90(60)[g]	3	90:10
3	(S_A,S_B,S_B)-**Lc**	90(88)[c](64)[g]	5	90:10
4	(S_A,S_B,S_B)-**Ld**	88(57)[g]	4	90:10
5	(R_A,S_B,S_B)-**La**	6	28	78:22
6	(R_A,S_B,S_B)-**Lb**	2	40	87:13
7	(R_A,S_B,S_B)-**Lc**	3	72(68)[c]	88:12
8	(R_A,S_B,S_B)-**Ld**	3	50	86:14
9[e]	(S_A,S_B,S_B)-**Lc**	90(62)[g]	4	89:11
10[f]	(S_A,S_B,S_B)-**Lc**	87(63)[g]	5	88:12
11[e]	(R_A,S_B,S_B)-**Lc**	5	70	83:17
12[f]	(R_A,S_B,S_B)-**Lc**	3	64	88:12

[a] Reaction conditions: **1a** (0.1 mmol), $Me_2C(OH)CN$ (0.3 mmol), $Ni(COD)_2$ (5 mol%), ligand (5 mol%), toluene (0.3 mL), 80 °C, 12 h. [b] Determined by GC analysis using *n*-decane as the internal standard. [c] Isolated yield. [d] rr is the regioisomeric ratio, which represents the ratio of the major product to the sum of all other isomers as determined by GC analysis. [e] Reactions conducted at 100 °C. [f] Reactions conducted at 60 °C. [g] The *ee* values were determined by HPLC over chiral stationary phase.

With two regioselective catalytic systems and optimized conditions established (Table 1, entries 3 and 7), we evaluated the substrate scope of this regiodivergent transformation (Scheme 3). Generally, the substituents on the aryl group mainly control the yield and regioselectivity of the branched nitrile product **2** but slightly affect the yield and regioselectivity of the linear nitrile product **3**. Substrates containing various functional groups such as ester (**1b**), nitrile (**1c**), phenol (**1e**), amine (**1f**), halogen (**1h**), ethers (**1i**, **1l**), boron (**1j**) and heterocycles such as indole (**1o**) and furan (**1p**), were examined. All were smoothly converted to the corresponding branched and linear nitriles in moderate to high yields with high regioselectivities. Furthermore, the alkene bearing an estrone skeleton (**1q**) was also successfully converted into the desired products **2q** and **3q** in

86% and 61% yield, respectively. Next, we studied an array of internal alkenes with various chain lengths. Under the standard conditions, the substrates with longer chain length afforded the desired products in lower yields, whereas the regioselectivity of the benzylic nitriles were uniformly *ca*. 90:10 (**1r**–**1u**). Evidently, the longer chain-walking distance between the double bond and the terminus makes the formation of linear nitriles more difficult. Thus, the conversion, yield and regioselectivity significantly decreased (**1v**–**1y**). It is worth mentioning that this migratory hydrocyanation features an enantioselective potential. By employing the Ni/(S_A,S_B,S_B)-**Lc** catalyst, branched nitriles could be obtained with moderate enantioselectivities. For example, the ee's of **2a**, **2c** and **2o** were 64%, 62% and 77% *ee* respectively. Remarkably, the employment of enantioselective chain-walking strategy to construct enantiomerically enriched molecules remains quite elusive in the previous report.

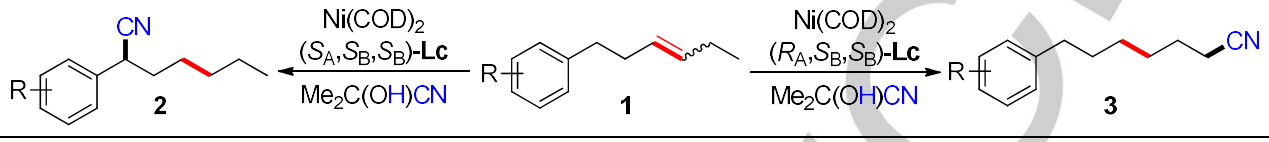

R=H, **2a**: 88% yield, 90:10 rr, 64% *ee*; **3a**: 68% yield, 88:12 rr
R=4-CO_2Et, **2b**: 68% yield, 89:11 rr; **3b**: 65% yield, 93:7 rr
R=4-CN, **2c**: 62% yield, 90:10 rr, 62% *ee*; **3c**: 53% yield, 93:7 rr
R=4-^{t}Bu, **2d**: 54% yield, 77:23 rr; **3d**: 62% yield, 91:9 rr
R=4-OH, **2e**: 95% yield, 98:2 rr; **3e**: 61% yield, 91:9 rr
R=4-NHAc, **2f**: 54% yield, 73:17 rr; **3f**: 52% yield, 82:18 rr
R=4-Ph, **2g**: 92% yield, 94:6 rr; **3g**: 56% yield, 88:12 rr
R=4-F, **2h**: 90% yield, 95:5 rr; **3h**: 58% yield, 92:8 rr
R=4-OMe, **2i**: 93% yield, 97:3 rr; **3i**: 61% yield, 87:13 rr
R=4-Bpin, **2j**: 76% yield, 90:10 rr; **3j**: 63% yield, 92:8 rr
R=2-Me, **2k**: 83% yield, 88:12 rr; **3k**: 63% yield, 93:7 rr
R=2-OMe, **2l**: 89% yield, 91:9 rr; **3l**: 70% yield, 86:14 rr

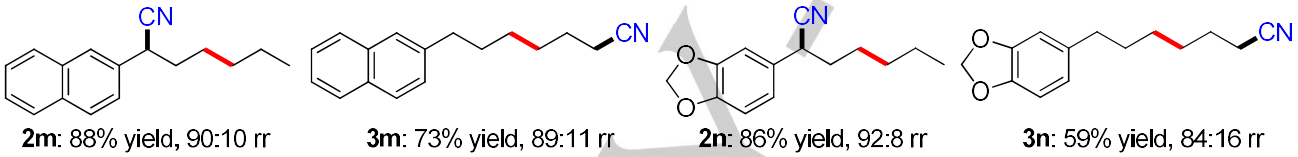

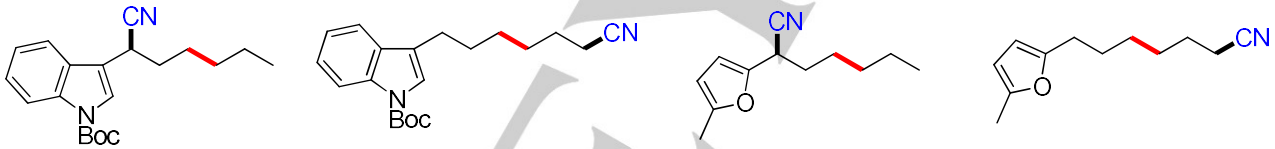

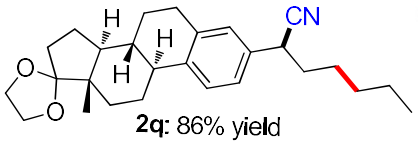

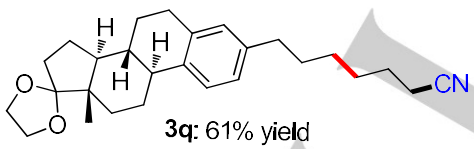

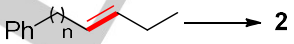

2r: n=1, 86% yield, 93:7 rr
2s: n=3, 82% yield, 88:12 rr
2t: n=4, 64% yield, 88:12 rr
2u: n=5, 42% yield, 89:11 rr

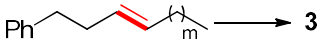

3v: m=0, 70% yield, 90:10 rr
3w: m=2, 65% yield, 82:18 rr
3x: m=3, 51% yield, 84:16 rr
3y: m=4, 40% yield, 80:20 rr

Scheme 3. Substrate scope of the regiodivergent hydrocyanation of various internal alkenes **1**. [a] Reaction conditions: **1** (0.2 mmol), $Me_2C(OH)CN$ (0.6 mmol), $Ni(COD)_2$ (5 mol%), ligand (5 mol%), toluene (0.5 mL), 80 °C, 12 h. Yields of the isolated products after flash column chromatography (single linear or branched product). rr, the regioisomeric ratio, represents the ratio of the major product to the sum of all other isomers as determined by GC analysis. The *ee* values were determined by HPLC over chiral stationary phase.

Another consequence of our methodology is the feasibility of the implemented regioconvergent hydrocyanation, which would allow inexpensive chemical feedstocks such as unrefined alkene isomers to be uniformly transformed to two different value-added products in a single step. On one hand, treatment of a 1:1:1:1 mixture of alkene regioisomers afforded **2a** in 81% yield with 89:11 regioselectivity on gram scale under standard conditions (Scheme 4). On the other hand, the terminal nitrile **3a** was obtained in 70% yield with 88:12 regioselectivity.

To gain further insight into this chain-walking process, some deuterium labeling experiments and crossover reactions were performed (Scheme 5). Fully deuterium-labeled acetone cyanohydrin was initially employed for the model reaction under standard conditions (Scheme 5a). We observed deuterium incorporation at the C1 (0.05D), C2-C5 (1.28D) and C6 (0.37D)

positions in **d-2n-1** in 83% yield with 92:8 rr, meanwhile C1 (0.40D), C2-C5 (1.64D) and C6 (0D) positions in **d-3n-1** in 58% yield with 85:15 rr. When deuterium-labeled **d-1z** was used as substrate instead (Scheme 5a), the corresponding benzylic nitrile **d-2z-1** was obtained with the deuterium atom incorporated at C1 (0.02D), C2 (0.36D), C3 (0.09D) and C4 (0.06D) in 78% yield with 93:7 rr, and the terminal nitrile **d-3z-1** was obtained with the deuterium atom incorporated at C1 (0.05D), C2 (0.12D), C3 (0.06D) and C4 (0.04D) in 50% yield with 79:21 rr. These two results collectively suggested a mechanism where the Ni catalyst walks along the carbon chain via an iterative *β*-H elimination and reinsertion processes. In order to determine whether H−Ni−CN remains ligated to the substrate throughout the chain-walking process, a mixture of **d-1z** and **1aa**/**1n** were subjected to the reaction (Scheme 4b), the hydrocyanation products **d-2z-2**, **d-2aa** and **d-3z-2**, **d-3n-2** were all deuterium labeled. If the chain-walking process would take place without dissociation of H−Ni−CN, the product **d-2aa** and **d-3n-2** would be detected without any deuterium labeling. Therefore, a mechanism in which chain-walking proceeds with the reassociation of H−Ni−CN is proposed.

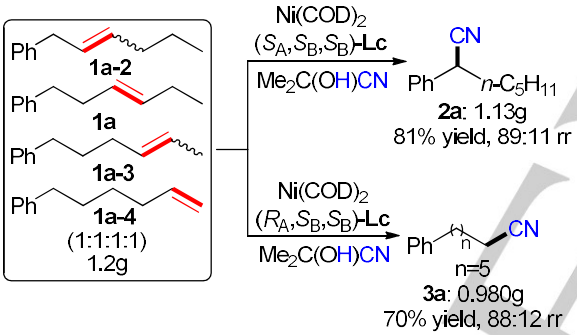

Scheme 4. Gram-scale regioconvergent experiment.

To understand the divergent regioselectivities obtained with the diastereomeric biaryl diphosphite ligands, we conducted density functional theory (DFT) calculations.[18] The simplest substrate **1z** and ligand **La** were used in the calculation to minimize the computational cost as substrate and ligand do not reverse the regioselectivity. As shown in Figure 1a, alkene migration of **1z** via sequential alkene insertion and *β*-hydride elimination will generate its isomers **1z-2** and **1z-3** which further undergo alkene insertion and reductive elimination to generate branched product **2z** and linear product **3z**, respectively.[19]

The computed free energy profiles for the reactions with (S_A,S_B,S_B)-**La** (Figure 1b and Figure S1) and (R_A,S_B,S_B)-**La** ligands (Figure S2) suggest that the alkene insertion and *β*-hydride elimination (**TS1**, **TS2**, and **TS3**) are facile and reversible processes with barriers lower than 13 kcal/mol. This indicates that the isomers **1z**, **1z-2** and **1z-3** are interconvertible via chain-walking process, in line with the deuterium labeling experiments. In both Ni/(S_A,S_B,S_B)-**La** and Ni/(R_A,S_B,S_B)-**La** systems, the reductive elimination step (**TS4**) was calculated to have the highest activation barrier and it is an irreversible step as it leads to a very stable hydrocyanation product. Thus, the reductive elimination step determines both the reaction rate and regioselectivity. For Ni/(S_A,S_B,S_B)-**La** system, the reductive elimination to form **2z** is more favorable than that for **3z** by 2.3 kcal/mol which is consistent with experimental results that **2z** is preferred over **3z**. While for Ni/(R_A,S_B,S_B)-**La** system, the formation of **3z** is more favored than **2z** via by 1.4 kcal/mol that is again in agreement with experimental results.

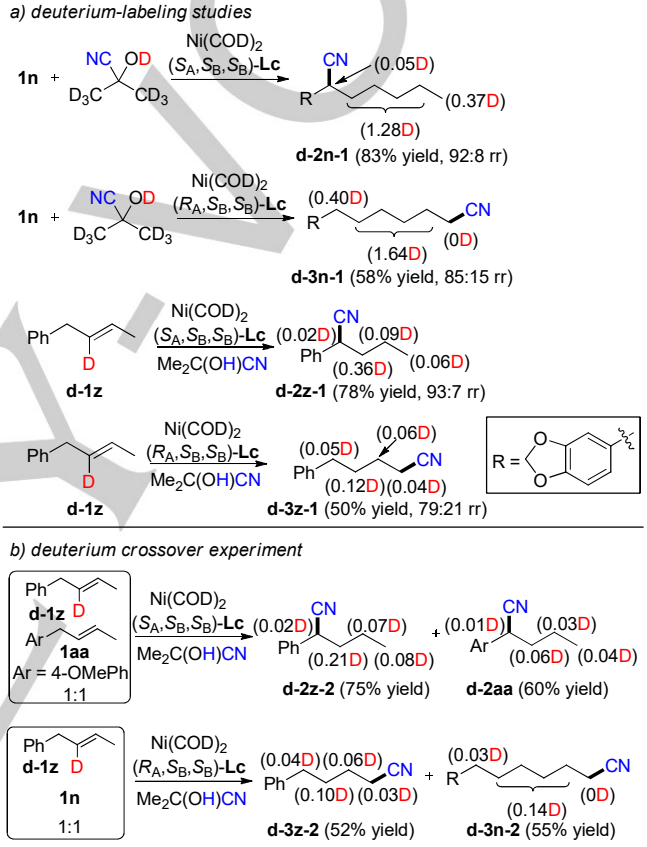

Scheme 5. Deuterium labeling experiments.

As shown in Figure 2, the optimized stuctures of Ni/(S_A,S_B,S_B)-**La** and Ni/(R_A,S_B,S_B)-**La** catalysts show very different features. The previous one has a more open pocket surrounding the Ni while the latter one features with a narrow pocket with Ni sandwiched between naphthalene rings. For Ni/(S_A,S_B,S_B)-**La** system with a large pocket, substrate could easily accommodate the pocket without obvious steric hindrance with ligand in the transition states of reductive elimination that generate **2z** and **3z**. But the reductive elimination at benzylic carbon is electronically more favorable due to the charge delocalization of **C1** by phenyl group which is indicated by a shorter bond length of 1.49 Å for **C1**-C_{phenyl} in **L1-TS4-1** compared with that in substrate (1.52 Å). Moreover, NBO analysis demonstrates that the binding of phenyl group to Ni in

L1-TS4-1 is stronger than the agostic interaction in **L1-TS4-2** by 3.6 kcal/mol (Figure S3). For Ni/(R_A,S_B,S_B)-**La** system, the substrate has to squeeze into the narrow pocket. As a result, **L2-TS4-1** suffers steric repulsions between the alkyl group of substrate and naphthalene ring and *tert*-butyl group of ligand (Figure 2) and the coordination of phenyl group with Ni is disrupted. By comparison, the substrate is relatively farther from the naphthalene rings of ligand and no obvious steric hindrance was detected in **L2-TS4-2**. In addition, a strong agostic interaction between substrate and Ni (d_{Ni-H} = 1.73 Å vs. 2.11 Å in **L2-TS4-1**) helps to stabilize **L2-TS4-2**. Therefore, our computational results suggest that the coordination of diastereomeric biaryl diphosphite ligands with Ni lead to dramatically different catalyst architectures which generate divergent regioselectivities by tuning the electronic and steric interactions.

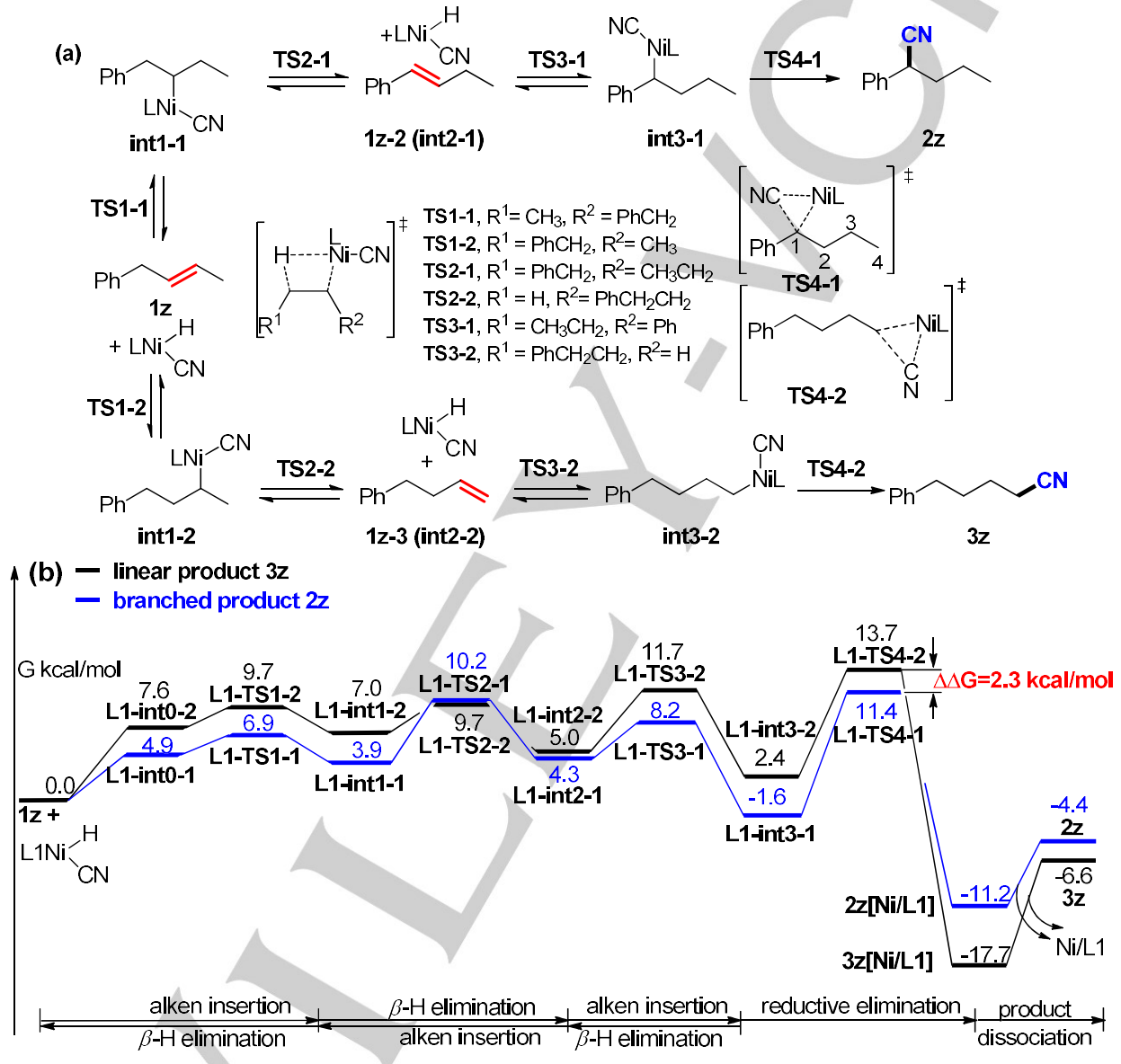

Figure 1. (a) Formation of branched product **2z** and linear product **3z** from Ni-catalyzed migratory hydrocyanation reaction. (b) Free energy profile of Ni-catalyzed migratory hydrocyanation of **1z** with ligand (S_A,S_B,S_B)-**La** (**L1**). Relative free energies are in kcal/mol.

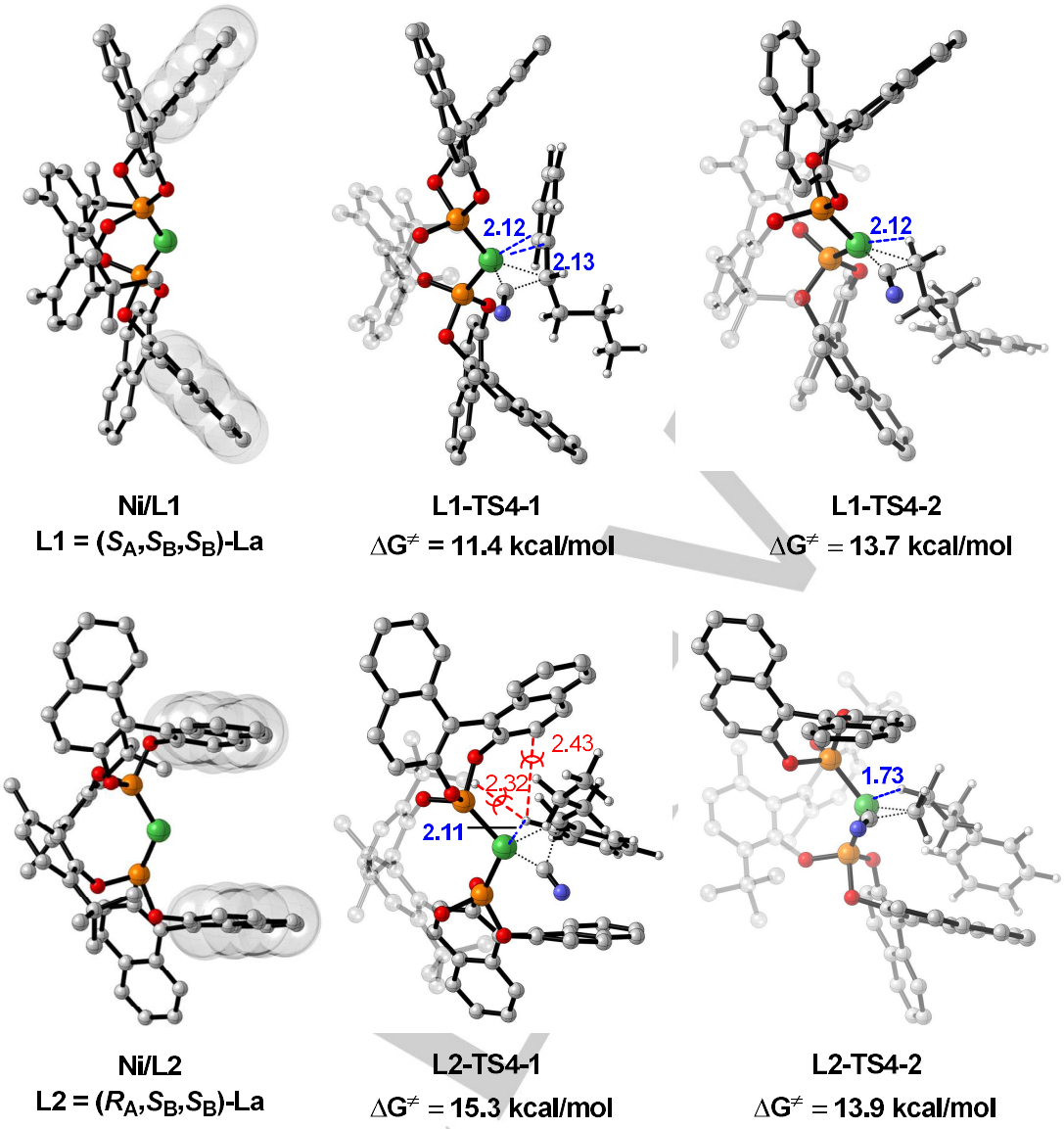

Figure 2. Optimized geometries of Ni/**La** catalysts and reductive elimination transition states. H atoms of ligands are emitted for clarity and distances are shown in Å. Distances in red and blue indicate repulsion and attractive binding interactions, respectively.

Conclusion

In summary, a generalized Ni-based catalytic platform that promotes robust and reliable regiodivergent migratory hydrocyanation of internal alkenes by the judicious choice of diastereomeric biaryl diphosphite ligands was developed. This protocol provides a wide range of linear or branched nitriles with good yields and regioselectivities from the same starting materials. DFT calculations suggested that the catalyst architecture determines the regioselectivity via modulating electronic and steric interactions. Additional work for the better mechanistic understanding of this process and further investigations on the development of highly enantioselective migratory hydrocyanation of internal alkenes are in progress.

Acknowledgements

The research was supported by the Recruitment Program of Global Experts, the startup funding from Shanghai Jiao Tong University, and the National Natural Science Foundation of China (21803047). The authors gratefully acknowledge Prof. Bill Morandi (ETH, Zürich) and Prof. Wanfang Li (University of Shanghai for Science and Technology) for inspiring discussions.

Conflict of interest

The authors declare no conflict of interest.

Keywords: regiodivergent catalysis • remote hydrocyanation • chain-walking • nickel catalysis • diastereomeric ligands

[1] For representative reviews, see: a) L.-W. Xu, L. Li, G.-Q. Lai, *Mini-Rev. Org. Chem.* **2007**, *4*, 217−230; b) N. Funken, Y.-Q. Zhang, *Chem. Eur. J.* **2017**, *23*, 19−32; c) I. P. Beletskaya, C. Nájera, M. Yus, *Chem. Rev.* **2018**, *118*, 5080−5200; d) Y.-C. Lee, K. Kumar, H. Waldmann, *Angew. Chem. Int. Ed.* **2018**, *57*, 5212−5226; e) C. Nájera, I. P. Beletskaya, M. Yus, *Chem. Soc. Rev.* **2019**, *48*, 4515−4618.

[2] For selected examples, see: a) Z. D. Miller, Dorel. R, J. Montgomery, *Angew. Chem. Int. Ed.* **2015**, *54*, 9088−9091; b) M. Li, M. Gonzalez-Esguevillas, S. Berritt, X. Yang, A. Bellomo, P. J. Walsh, *Angew. Chem. Int. Ed.* **2016**, *55*, 2825−2829; c) X. Du, Y. Zhang, D. Peng, Z. Huang, *Angew. Chem. Int. Ed.* **2016**, *55*, 6671−6675; d) G. Xu, H. Zhao, B. Fu, A. Cang, G. Zhang, Q. Zhang, T. Xiong, Q. Zhang, *Angew. Chem. Int. Ed.* **2017**, *56*, 13130−13134; e) S. R. Sardini, M. K. Brown, *J. Am. Chem. Soc.* **2017**, *139*, 9823−9826; f) W. Liu, W. Ren, J. Li, Y. Shi, W. Chang, Y. Shi, *Org. Lett.* **2017**, *19*, 1748–1751; g) T. Shimbayashi, G. Matsushita, A. Nanya, A. Eguchi, K. Okamoto, K. Ohe, *ACS Catal.* **2018**, *8*, 7773−7780; h) D. Bai, X. Wang, G. Zheng, X. Li, *Angew. Chem. Int. Ed.* **2018**, *57*, 6633−6637; i) Z. Zeng, H. Jin, M. Rudolph, F. Rominger, A. S. K. Hashmi, *Angew. Chem. Int. Ed.* **2018**, *57*, 16549−16553; j) W. Li, J. K. Boon, Y. Zhao, *Chem. Sci.* **2018**, *9*, 600−607; k) F. Wang, D. Wang, Y. Zhou, L. Liang, R. Lu, P. Chen, Z. Lin, G. Liu, *Angew. Chem. Int. Ed.* **2018**, *57*, 7140−7145; l) Y. Li, H. Wei, D. Wu, Z. Li, W. Wang, G. Yin, *ACS Catal.* **2020**, *10,* 4888−4894.

[3] For selected examples, see: a) A. Seayad, M. Ahmed, H. Klein, R. Jackstell, T. Gross, M. Beller, *Science* **2002**, *297*, 1676–1678; b) E. W. Werner, T.-S. Mei, A. J. Burckle, M. S. Sigman, *Science* **2012**, *338,* 1455–1458; c) T.-S. Mei, H. H. Patel, M. S. Sigman, *Nature* **2014**, *508*, 340–344; d) A. Masarwa, D. Didier, T. Zabrodski, M. Schinkel, L. Ackermann, I. Marek, *Nature* **2014**, *505*, 199–203; e) T. Hamasaki, Y. Aoyama, J. Kawasaki, F. Kakiuchi, T. Kochi, *J. Am. Chem. Soc.* **2015**, *137*, 16163–16171; f) L. Mola, M. Sidera, S. P. Fletcher, *Aust. J. Chem.* **2015**, *68*, 401–403; g) S. Dupuy, K.-F. Zhang, A.-S. Goutierre, O. Baudoin, *Angew. Chem. Int. Ed.* **2016**, *55*, 14793–14797; h) Y. He, Y. Cai, S. Zhu, *J. Am. Chem. Soc.* **2017**, *139*, 1061–1064; i) Y. Ebe, M. Onoda, T. Nishimura, H. Yorimitsu, *Angew. Chem. Int. Ed.* **2017**, *56*, 5607–5611; j) A. J. Borah, Z. Shi, *J. Am. Chem. Soc.* **2018**, *140*, 6062–6066; k) Z.-Y. Wang, J.-H. Wan, G.-Y. Wang, R. Wang, R.-X. Jin, Q. Lan, X.-S. Wang, *Tetrahedron Lett.* **2018**, *59*, 2302–2305; l) C. Romano, C. Mazet, *J. Am. Chem. Soc.* **2018**, *140*, 4743–4750; m) L. Zhou, C. Zhu, P. Bi, C. Feng, *Chem. Sci.* **2019**, *10*, 1144–1149; n) S.-Z. Sun, C. Romano, R. Martin, *J. Am. Chem. Soc.* **2019**, *141*, 16197–16201; o) Y. Gao, C. Yang, S. Bai, X. Liu, Q. Wu, J. Wang, C. Jiang, X. Qi, *Chem* **2020**, *6*, 675–688.

[4] For selected examples, see: a) J. V. Obiligacion, P. J. Chirik, *J. Am. Chem. Soc.* **2013**, *135*, 19107–19110; b) X. Chen, Z. Cheng, J. Guo, Z. Lu, *Nat. Commun.* **2018**, *9*, 3939; c) F. Zhou, Y. Zhang, X. Xu, S. Zhu, *Angew. Chem. Int. Ed.* **2019**, *58*, 1754–1758; d) C. Romano, D. Fiorito, C. Mazet, *J. Am. Chem. Soc.* **2019**, *141*, 16983–16990; e) W. Wang, C. Ding, Y. Li, Z. Lin, L. Peng, G. Yin, *Angew. Chem. Int. Ed.* **2019**, *58*, 4612–4616; f) C. Matt, C. Kern, J. Streuff, *ACS Catal.* **2020**, *10*, 6409–6413; g) M. Hu, S. Ge, *Nat. Commun.* **2020**, *11*, 765; h) J. Li, S. Qu, W. Zhao, *Angew. Chem. Int. Ed.* **2020**, *59*, 2360–2364.

[5] B. Liu, P. Hu, F. Xu, L. Cheng, M. Tan, W. Han, *Commun. Chem.* **2019**, *2*, 5–13.

[6] I. Buslov, J. Becouse, S. Mazza, M. Montandon-Clerc, X. Hu, *Angew. Chem. Int. Ed.* **2015**, *54*, 14523–14526.

[7] Y. Zhang, X. Xu, S. Zhu, *Nat. Commun.* **2019**, *10*, 1752.

[8] For selected examples, see: a) D. M. Ohlmann, L. J. Goosen, M. Dierker, *Chem. Eur. J.* **2011**, *17*, 9508–9519; b) D. G. Kohler, S. N. Gockel, J. L. Kennemur, P. J. Waller, K. L. Hull, *Nat. Chem.* **2018**, *10*, 333–341; c) J. Xiao, Y. He, F. Ye, S. Zhu, *Chem* **2018**, *4*, 1645–1657; d) C. Han, Z. Fu, S. Guo, X. Fang, A. Lin, H. Yao, *ACS Catal.* **2019**, *9*, 4196–4202.

[9] For selected reviews on alkene chain-walking functionalizations, see: a) M. Domke, L. Vilches-Herrera, A. Börner, *ACS Catal*. **2014**, *4*, 1706−1724; b) A. Vasseur, J. Bruffaerts, I. Marek, *Nat. Chem.* **2016**, *8*, 209−219; c) T. Kochi, S. Kanno, F. Kakiuchi, *Tetrahedron Lett.* **2019**, *60*, 150938−150950; d) Y. Li, D. Wu, H.-G. Cheng, G. Yin, *Angew. Chem. Int. Ed*. **2020**, *59*, 7990−8003; e) I. Massad, I. Marek, *ACS Catal*. **2020**, *10*, 5793−5804.

[10] a) W.-C. Lee, C.-H. Wang, Y.-H. Lin, W.-C. Shih, T.-G. Ong, *Org. Lett.* **2013**, *15*, 5358−5361; b) W.-C. Lee, C.-H. Chen, C.-Y. Liu, M.-S. Yu, Y.-H. Lin, T.-G. Ong, *Chem. Commun*. **2015**, *51*, 17104−17107; c) M. L. Scheuermann, E. J. Johnson, P. J. Chirik, *Org. Lett.* **2015**, *17*, 2716–2719; d) F. Juliá-Hernández, T. Moragas, J. Cornella, R. Martin, *Nature* **2017**, *545*, 84–88; e) D. Qian, X. Hu, *Angew. Chem. Int. Ed*. **2019**, *58*, 18519−18523; f) X. Yu, H. Zhao, S. Xi, Z. Chen, X. Wang, L. Wang, L. Q. H. Lin, K. P. Loh, M. J. Koh, *Nat. Catal*. **2020**, *3*, 585−592; g) C. Yang, Y. Gao, S. Bai, C. Jiang, X. Qi, *J. Am. Chem. Soc.* **2020**, *142*, 11506−11513.

[11] For selected reviews, see: a) H. Fernández-Pérez, P. Etayo, A. Panossian, A. Vidal-Ferran, *Chem. Rev.* **2011**, *111*, 2119−2176; b) P. W. N. M. van Leeuwen, P. C. J. Kamer, C. Claver, O. Pàmies, M. Diéguez, *Chem. Rev.* **2011**, *111*, 2077–2188.

[12] For selected reviews, see: a) K. Muñiz, C. Bolm, *Chem. Eur. J.* **2000**, *6*, 2309–2316; b) C. J. Richards, R. A. Arthurs, *Chem. Eur. J.* **2017**, *23*, 11460–11478. Selected examples, see: c) L. Qiu, J. Qi, C.-C. Pai, S. Chan, Z. Zhou, M. C. K. Choi, A. S. C. Chan, *Org. Lett.* **2002**, *4*, 4599−4602; d) W.-J. Shi, Q. Zhang, J.-H. Xie, S.-F. Zhu, G.-H. Hou, Q.-L. Zhou, *J. Am. Chem. Soc.* **2006**, *128*, 2780−2781; e) E. Cesarotti, G. Abbiati, E. Rossi, P. Spalluto, I. Rimoldi, *Tetrahedron: Asymmetry* **2008**, *19*, 1654–1659; f) X. Sun, W. Li, L. Zhou, X. Zhang, *Chem. Eur. J.* **2009**, *15*, 7302–7305; g) C. You, S. Li, X. Li, J. Lan, Y. Yang, L. W. Chuang, H. Lv, X. Zhang, *J. Am. Chem. Soc.* **2018**, *140*, 4977−4981; h) R. A. Arthus, D. L. Hughes, C. J. Richards, *J. Org. Chem.* **2020**, *85*, 4838–4847.

[13] For selected reviews, see: a) M. Beller, J. Seayad, A. Tillack, H. Jiao, *Angew. Chem. Int. Ed.* **2004**, *43*, 3368–3398; b) L. Bini, C. Müller, D. Vogt, *ChemCatChem* **2010**, *2*, 590–608; c) L. Bini, C. Müller, D. Vogt, *Chem. Commun.* **2010**, *46*, 8325–8334; d) T. V. RajanBabu, *Org. React.* **2011***, 75*, 1–73; e) N. Kurono, T. Ohkuma, *ACS Catal.* **2016**, *6*, 989–1023; f) H. Zhang, X. Su, K. Dong, *Org. Biomol. Chem.* **2020**, *18*, 391−399; g) W.-B. Wu, J.-S. Yu, J. Zhou, *ACS Catal.* **2020**, *10*, 7668–7690.

[14] For selected examples, see: a) A. L. Casalnuovo, T. V. RajanBabu, T. A. Ayers, T. H. Warren, *J. Am. Chem. Soc.* **1994**, *116*, 9869−9882; b) M. Yan, Q.-Y. Xu, A. S. C. Chan, *Tetrahedron: Asymmetry* **2000**, *11*, 845−849; c) W. Goertz, P. C. J. Kamer, P. W. N. M. van Leeuwen, D. Vogt, *Chem. Eur. J.* **2001**, *7*, 1614−1618; d) B. Saha, T. V. RajanBabu, *Org. Lett.* **2006**, *8*, 4657−4659; e) J. Wilting, M. Janssen, C. Müller, D. Vogt, *J. Am. Chem. Soc.* **2006**, *128*, 11374−11375; f) J. Wilting, M. Janssen, C. Müller, M. Lutz, A. L. Spek, D. Vogt, *Adv. Synth. Catal.* **2007**, *349*, 350−356; g) M. de Greef, B. Breit, *Angew. Chem. Int. Ed.* **2009**, *48*, 551–554; h) A. Falk, A.-L. Göderz, H.-G. Schmalz, *Angew. Chem. Int. Ed.* **2013**, *52*, 1576−1580; i) A. Falk, A. Cavalieri, G. S. Nichol, D. Vogt, H.-G. Schmalz, *Adv. Synth. Catal.* **2015**, *357*, 3317−3320; j) K. Nemoto, T. Nagafuchi, K. Tominaga, K. Sato, *Tetrahedron Lett.* **2016**, *57*, 3199−3203; k) X. Fang, P. Yu, B. Morandi, *Science* **2016**, *351*, 832−836; l) B. N. Bhawal, J. C. Reisenbauer, C. Ehinger, B. Morandi, *J. Am. Chem. Soc.* **2020**, *142*, 10914−10920; m) N. L. Frye, A. Bhunia, A. Studer, *Org. Lett*. **2020**, *22*, 4456−4460; n) L. Song, N. Fu, B. G. Ernst, W. H. Lee, M. O. Frederick, R. A. DiStasio, S. Lin, *Nat. Chem.* **2020**, *12*, 747−754; o) J. Long, R. Yu, J. Gao, X. Fang, *Angew. Chem. Int. Ed*. **2020**, *59*, 6785–6789; p) R. Yu, X. Fang, *Org. Lett.* **2020**, *22*, 594–597; q) J. Gao, J. Long, X. Fang, *Org. Lett.* **2020**, *22*, 376–380; r) Y. Xing, R. Yu, X. Fang, *Org. Lett.* **2020**, *22*, 1008–

1012; s) R. Yu, S. Rajasekar, X. Fang, *Angew. Chem. Int. Ed.* **2020**, *59*, doi.org/10.1002/anie.202008854.

[15] A. Bhunia, K. Bergander, A. Studer, *J. Am. Chem. Soc.* **2018**, *140*, 16353−16359.

[16] G. Wang, X. Xie, W. Xu, Y. Liu, *Org. Chem. Front.* **2019**, *6*, 2037−2042.

[17] X. Shu, Y.-Y. Jiang, L. Kang, L. Yang, *Green Chem.* **2020**, *22*, 2734−2738.

[18] Details of the computational method, energies and geometry information are provided in supporting information.

[19] Other branched isomeric products could be generated via direct reductive eliminations of **int1-1** and **int1-2** which are also considered in computational study as shown in supporting information.

10.1002/anie.202011231

WILEY-VCH

RESEARCH ARTICLE

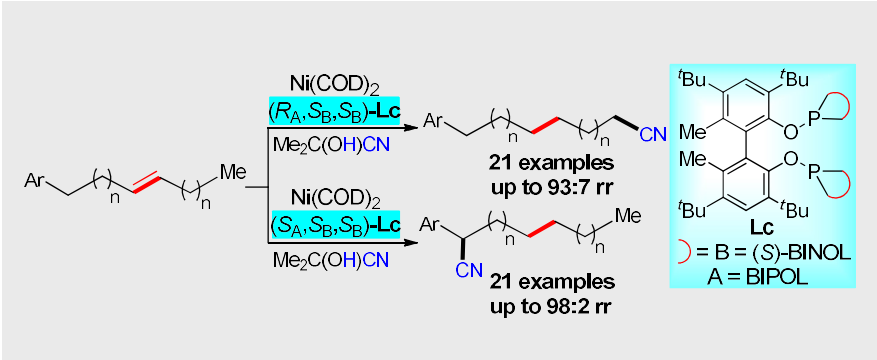

J. Gao⁺, M. Jiao⁺, J. Ni⁺, R. Yu, G.-J. Cheng, X. Fang**

Nickel-Catalyzed Migratory Hydrocyanation of Internal Alkenes: Unexpected Diastereomeric-Ligand-Controlled Regiodivergence

The use of diastereomeric ligands has now allowed the regiodivergent chain-walking hydrocyanation of internal alkenes. The reactions provided a wide range of linear or branched nitriles with good yields and regioselectivities from the same reactants. DFT calculations suggested that the catalyst architecture determines the regioselectivity via the modulation of electronic and steric interactions.